JOURNAL OF PHYSICAL ORGANIC CHEMISTRY, VOL. 11, 241–253 (1998)

Conformational analysis of a 12-membered crown dithioether in the solid state and in solution

Vyacheslav V. Samoshin,[1]*‡ Emmanuil I. Troyansky,[2] Dmitry V. Demchuk,[2] Rustem F. Ismagilov,[2] Vyacheslav A. Chertkov,[3] Sergei V. Lindeman,[4] Victor N. Khrustalyov[4] and Yury T. Struchkov,[4]†

[1]Lomonosov Moscow State Academy of Fine Chemical Technology, Vernadsky Prospekt 86, Moscow, 117571, Russia
[2]Zelinsky Institute of Organic Chemistry, Russian Academy of Sciences, Leninsky Prospekt 47, Moscow, 117334, Russia
[3]Department of Chemistry, Lomonosov Moscow State University, Moscow, 119899, Russia
[4]Nesmeyanov Institute of Organoelement Compounds, Russian Academy of Sciences, Vavilova St. 28, Moscow 117334, Russia

Received 22 May 1997; revised 20 August 1997; accepted 29 September 1997

ABSTRACT: The solid-state molecular structure and the conformational behaviour in solution of the 12-membered crown dithioether 8-methyl-1,4-dioxa-7,10-dithiacyclododecane-5,12-dione were studied by x-ray crystallography, ^{1}H and ^{13}C NMR spectroscopy and molecular mechanics. The conformational rigidity of some constituent structural fragments allowed a detailed analysis of the structure and distribution of the conformers. A protocol for studies of multiconformational equilibrium was developed by means of the combined use of structure calculations and dynamic NMR measurements. © 1998 John Wiley & Sons, Ltd.

KEYWORDS: Crown dithioether; conformational analysis; multicomponent equilibrium

INTRODUCTION

The potential importance of and increased interest in the coordination chemistry of crown thioethers as complexing agents in analytical chemistry, medicine and environmental protection have led to extensive studies of their chelating ability in recent years.[1–4] Owing to the strong dependence of complexation on ligand structure and conformation, the structural peculiarities of cyclic polythioethers are of considerable interest. The conformational properties of crown thioethers are essentially different from those of oxygen analogues. Structural data on a variety of thiacrowns revealed a tendency for the CS—CC units to prefer a *gauche* conformation and for the SC—CS and SC—CC units to adopt an *anti* conformation, whereas in oxacrowns the analogous CO—CC and OC—CO fragments have a strong preference for *anti* and *gauche* conformations, respectively (for reviews, see Refs 1b–f). Almost all these data were obtained by x-ray crystal structure analysis, so the conformational properties of extremely flexible sulfur-containing macrocycles in solution can still be considered as *terra incognita*. In recent years, intensive and fruitful studies have been carried out in this field by means of molecular mechanics calculations[3,4,5a] and by NMR measurements combined with molecular dynamics simulations[2] or molecular mechanics calculations.[5b–d] However, taking into account the considerable interest in the structure-dependent complexation of late transition metal ions with polythioethers, additional efforts in this area are desirable.

In this work, we undertook a detailed study of the macrocycle conformations of the 12-membered crown dithioether 8-methyl-1,4-dioxa-7,10-dithiacyclododecane-5,12-dione (**1**), including x-ray crystal structure analysis, molecular mechanics calculations and NMR measurements.

RESULTS AND DISCUSSION

The crown thioether **1** was synthesized from ethylene glycol bis(mercaptoacetate) and methylacetylene by one-step homolytic cycloaddition.[6]

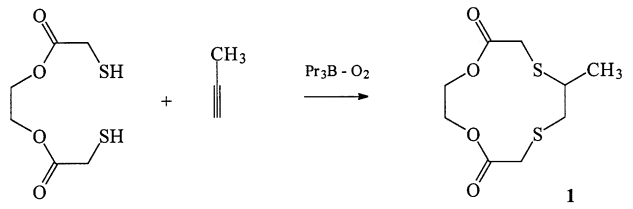

1

‡Now on leave at Department of Chemistry, University of the Pacific, Stockton, CA 95211, USA.
†Deceased.
**Correspondence to:* V. V. Samoshin, Department of Chemistry, University of the Pacific, Stockton, CA 95211, USA.
Contract/grant sponsor: INTAS; *contract grant number:* 94-1914.
Contract/grant sponsor: Russian Foundation for Basic Research; *contract grant number:* 94-03-09296.

CCC 0894–3230/98/040241–13 $17.50

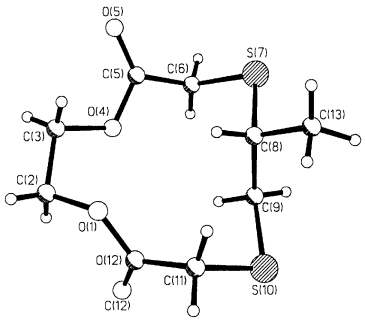

Figure 1. Molecular structure of **1**

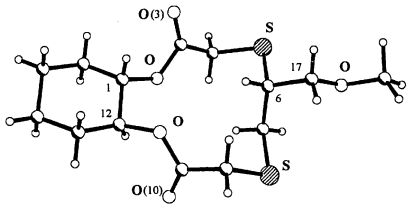

Figure 2. Molecular structure of **2**[5a]

X-ray analysis

The molecular structure of the macrocycle **1** in the solid state was unambiguously established from x-ray crystallographic data (Fig. 1 and Tables 1–5; see Experimental section). Although slightly less symmetrical, it closely resembles the structure of the macrocycle in the *trans*-cyclohexane-fused 12-membered crown thialactone **2** (Fig. 2).[5a]

Molecular packing in the crystal is stacked along the *Y*-axis (Fig. 3). The *R*- and *S*- enantiomers of **1** alternate along the *z*-axis. The molecules are separated by the usual van der Waals distances. It is interesting that owing to the tendency for the most compact packing, the crystal structure of **1** has no intermolecular contacts as weak hydrogen bonds C— H...O, unlike the crystal structure of **2** studied earlier.[5a]

Molecular mechanics calculations

To establish whether the conformation of **1** in the crystal form is the most stable, we calculated the relative energies of the conformers of macrocycle **1** by molecular mechanics (MMX force field, PCMODEL 3.2 program[7]). To achieve the complete screening of all possible conformers of macrocycle, we started calculations from the known conformers of cyclododecane:[8] we reconstructed their geometry, placed sulfur and oxygen atoms, and the carbonyl group in all of the 12 possible positions within the cycle and then minimized the energy of molecule. The first 20 most stable conformers of cyclododecane[8] within 5.5 kcal mol^{-1} from the global energy minimum were used as starting points. Several

Table 1. Experimental data for the crystallographic analysis of 8-methyl-1,4-dioxa-7,10-dithiacyclododecane-5,12-dione (**1**)

Crystal data	
Empirical formula	$C_9H_{14}O_4S_2$
Color, habit	Colorless needles
Crystal size (mm)	$0.2 \times 0.2 \times 0.4$
Crystal system	Monoclinic
Space group	$P2_1/c$
Unit cell dimensions	$a = 14.12(2)$ Å, $b = 5.513(7)$ Å, $c = 14.95(4)$ Å, $\beta = 97.44(2)^o$
Volume	1155.4 Å^3
Z	4
Formula weight	250.3
Density (calc.)	1.440 mgm^{-3}
Absorption coefficient	0.453 mm^{-1}
$F(000)$	528
Data collection	
Diffractometer used	Siemens P3/PC
Radiation	Mo K ($\lambda = 0.71073$ Å)
Temperature (K)	293
Monochromator	Highly oriented graphite crystal
2θ range	4.0–50.0^o
Scan type	$\omega/2\theta$
Scan speed	Variable; 3.08–29.30^o min^{-1} in ω
Scan range (ω)	2.00^o
Background measurement	Stationary crystal and stationary counter at the beginning and at the end of scan, each for 12.5% of total scan time
Standard reflections	Two measured every 98 reflections
Index ranges	$0 \le h \le 17$, $0 \le k \le 6$, $-18 \le l \le 18$
Reflections collected	2352
Independent reflections	2258 ($R_{int} = 10.74$ %)
Observed reflections	1315 [$F > 5.0\ \sigma\ (F)$]
Absorption correction	Not applied
Solution and refinement[a]	
System used	Siemens SHELXTL PLUS (PC Version)[17]
Solution	Direct methods
Refinement method	Full-matrix least-squares
Quantity minimized	$\Sigma w(F_o - F_c)^2$
Absolute structure	Not applied
Extinction correction	Not applied
Hydrogen atoms	Objectively found, refined isotropically
Weighting scheme	$w^{-1} = \sigma^2(F) + 0.0046F^2$
Number of parameters refined	192
Final R indices (obs. data)	$R = 7.45\%$, $wR = 10.18\%$
R indices (all data)	$R = 14.35\%$, $wR = 23.60\%$
Goodness-of-fit	1.34 H
Largest and mean Δ/σ	0.081, 0.024
Data-to-parameter ratio	6.8:1
Largest difference peak	0.69 e Å^{-3}
Largest difference hole	−0.56 e Å^{-3}

[a] The refinement of the structure was ended with relatively high R values and a considerable amount of the resting electron density due to the low quality of the crystal studied.

Table 2. Atom coordinates ($\times 10^4$) and isotropic displacement coefficients of **1** ($Å^2 \times 10^3$)

Atom	*x*	*y*	*z*	*U* (eq)[a]
O(1)	1599(3)	6469(8)	9606(3)	33(1)
O(4)	1210(3)	6526(7)	7764(3)	30(1)
O(5)	1456(4)	9554(8)	6813(3)	42(2)
O(12)	1334(3)	2469(9)	9728(4)	42(2)
S(7)	3407(1)	5976(3)	6978(1)	37(1)
S(10)	3537(1)	1791(3)	9557(1)	37(1)
C(2)	646(5)	6882(15)	9166(5)	34(2)
C(3)	708(6)	8142(13)	8299(5)	33(2)
C(5)	1562(5)	7468(12)	7044(4)	29(2)
C(6)	2136(6)	5604(13)	6626(5)	32(2)
C(8)	3565(5)	5383(14)	8196(5)	36(2)
C(9)	3260(6)	2768(13)	8379(5)	35(2)
C(11)	2910(6)	4045(13)	10136(5)	35(2)
C(12)	1862(5)	4141(12)	9809(4)	29(2)
C(13)	4606(6)	5928(17)	8539(6)	44(3)

[a] Equivalent isotropic *U* is defined as one third of the trace of the orthogonalized U_{ij} tensor.

new conformers of cyclododecane within these energy limits were generated during this search and also used in further calculations. They differed very slightly in geometry from conformers described by Goto.[8] 'Isomerism' of this kind has been already discussed in detail[8] and very likely arises from the peculiarities of the force field used in PCMODEL. Thus the number of calculated conformers of the unsubstituted 12-membered crown thialactone 1,4-dioxa-7,10-dithiacyclododecane-5,12-dione exceeded 240, although some of them were equivalent. The most stable forms were generated several times independently starting from various cyclododecane conformations. The conformers of **1** were obtained by attachment of a methyl group to the appropriate position of the S—C—C—S fragment and subsequent optimization of the molecular geometry. This operation quadrupled the number of calculated conformers, which amounted to 1000. Again, many of them appeared to be identical, and the most stable ones were obtained several times starting from various forms of unsubstituted macrocycle.

The procedure described above affords both *R*- and *S*-enantiomers of **1**. For the sake of comparability, we 'inverted' all *R*-forms into their mirror images and considered only the set of *S*-enantiomers (Fig. 4, Table 6).

Twenty of the most stable conformers of **1** are depicted in Fig. 4 with corresponding energy values in kcal mol^{-1} relative to the global energy minimum (within 1.90 kcal mol^{-1} from the last one). In contrast to **2**, their energies present a continuous sequence without pronounced interruptions. The relative energies of the first 60 conformers within 4 kcal mol^{-1} from the global minimum allowed us to calculate their population using a Boltzmann distribution: the most stable conformer occupied 22.6% and the first 28 conformers covered 95% of the total. These 28 most stable structures were used in all further considerations (Table 6).

The x-ray determined geometry of the macrocycle was also used as a starting point for molecular mechanics optimization. It allowed us to obtain only the conformer **1/8** (Fig. 4).

The conformers closely related to the x-ray determined structure of **1** are placed in the boxes in Fig. 4. After completion of the search and consideration of possible conformers of **1**, it is important to note that the crystal structure's image is not the most stable form as might be expected. It exceeds the global energy minimum at least by 1.28 kcal mol^{-1} (the eighth place in the sequence). The calculated population of all three conformers similar to the x-ray structure (**1/8, 1/13** and **1/15**) is 6.5%. Probably the conformer displayed in Fig. 1 is preferable in the crystal form owing to a higher level of symmetry of the macrocycle. Note that the conformer observed in the crystalline state is not the calculated lowest energy conformer also for **2**,[5a] or for 1,4,7-trithiacyclodecane.[4]

NMR measurements

Within the framework of the discrete conformational analysis approach, when the conformational equilibrium is fast on the NMR time-scale only one set of signals can be observed with the averaged parameters depending on

Table 3. Bond lengths (Å)

O(1)— C(2)	1.438(9)	S(10)— C(9)	1.834(8)
O(1)— C(12)	1.359(8)	S(10)— C(11)	1.811(9)
O(4)— C(3)	1.44(1)	C(2)— C(3)	1.48(1)
O(4)— C(5)	1.348(9)	C(5)— C(6)	1.50(1)
O(5)— C(5)	1.204(8)	C(8)— C(9)	1.54(1)
O(12)— C(12)	1.182(9)	C(8)— C(13)	1.52(1)
S(7)— C(6)	1.815(9)	C(11)— C(12)	1.50(1)
S(7)— C(8)	1.836(8)		

Table 4. Bond angles (°)

O(1)— C(2)— C(3)	108.5(6)	S(7)— C(8)— C(9)	110.0(5)
O(1)— C(12)— C(11)	109.6(6)	S(7)— C(8)— C(13)	106.7(6)
O(1)— C(12)— O(12)	124.3(6)	C(6)— S(7)— C(8)	104.8(4)
O(4)— C(3)— C(2)	106.5(6)	S(7)— C(6)— C(5)	111.7(5)
O(4)— C(5)— O(5)	123.5(6)	C(9)— C(8)— C(13)	113.9(6)
O(4)— C(5)— C(6)	110.2(6)	C(8)— C(9)— S(10)	114.6(5)
O(5)— C(5)— C(6)	126.2(7)	C(9)— S(10)— C(11)	101.6(4)
C(2)— O(1)— C(12)	117.6(5)	S(10)— C(11)— C(12)	113.1(5)
C(3)— O(4)— C(5)	117.6(5)	C(11)— C(12)— O(12)	126.1(6)

Table 5. Hydrogen coordinates ($\times 10^3$) and isotropic displacement coefficients (Å$^2 \times 10^2$)

Atom	*x*	*y*	*z*	*U*
H(2)a	36(4)	771(11)	951(4)	0(1)
H(2)b	33(4)	548(11)	907(3)	0(1)
H(3)a	12(5)	840(10)	796(4)	2(2)
H(3)b	105(5)	934(15)	833(5)	4(2)
H(6)a	192(5)	423(13)	668(4)	3(2)
H(6)b	211(4)	574(10)	601(4)	1(1)
H(8)a	316(5)	645(11)	843(4)	2(2)
H(9)a	256(4)	245(11)	820(4)	2(2)
H(9)b	358(6)	175(16)	799(6)	6(3)
H(11)a	330(5)	555(13)	1008(4)	3(2)
H(11)b	296(5)	354(13)	1074(5)	4(2)
H(13)a	508(7)	446(20)	835(6)	9(3)
H(13)b	481(6)	769(17)	850(6)	5(2)
H(13)c	464(5)	580(14)	921(6)	5(2)

both the parameters of individual conformers and their population. It is common practice to use spin–spin coupling constants for the evaluation of conformer distributions. To describe the equilibrium between *M* conformers one has to compose a linear system of $N+1$ equations with *M* unknowns [$(N]+1) \geq M$]:

$$\begin{aligned} J_a^{exp} &= J_a{}^1 n^1 + J_a{}^2 n^2 + \ldots + J_a{}^M n^M \\ J_b^{exp} &= J_b{}^1 n^1 + J_b{}^2 n^2 + \ldots + J_b{}^M n^M \\ J_c^{exp} &= J_c{}^1 n^1 + J_c{}^2 n^2 + \ldots + J_c{}^M n^M \qquad (1) \\ &\vdots \\ J_z^{exp} &= J_z{}^1 n^1 + J_z{}^2 n^2 + \ldots + J_z{}^M n^M \\ 1 &= n^1 + n^2 + \ldots + n^M \end{aligned}$$

In the case when $N+1 \geq$ M, the population of all *M* conformers (n^i) can be evaluated on the basis of *N* experimentally measured spin couplings ($J_a^{exp.}$, $J_b^{exp.}$, ... , J_z^{exp}.), provided the corresponding parameters of each conformer are known. The enormous number of possible conformations of macrocycle **1** cause major complications with this approach. We attempted to solve this problem by using the maximum set of measurable vicinal proton–proton and carbon–proton spin–spin coupling constants $^3J_{HH}$ and $^3J_{CH}$.

The most obvious initial information can be obtained from the spin–spin coupling of vicinal hydrogens in $SCHMeCH_2S$ moiety. These values measured in the ^{1}H NMR spectra (400 MHz, C_6D_{12} solution) for vicinal hydrogen atoms in the $SCHMeCH_2S$ moiety are 4.78 Hz [$J_{H(8t)H(9t)}$] and 10.02 Hz [$J_{H(8t)H(9c)}$] (see Schemes 1 and 2), pointing to a preference for the *anti* conformation of S—C—C—S fragment in solution (Scheme 2, conformer **A**). The same preference was observed earlier for some crown thioethers.[1–5] The role of the other rotamers participating in the equilibrium increases with the solvent polarity: the couplings are 4.84 and 10.17 Hz in C_6D_6, 4.94 and 9.63 Hz in $CDCl_3$ and 5.19 and 9.53 Hz in CD_3OD. The corresponding individual vicinal couplings for the first 28 conformers (see above) were calculated by the PCMODEL program (Table 7) and then averaged with Boltzmann weight factors resulting in 5.84 and 7.93 Hz for $J_{H(8t)H(9t)}$ and $J_{H(8t)H(9c)}$], respectively. These values are only in rough agreement with the experimental values. A similar averaging procedure was used earlier for spin couplings in nitrogen-containing five-membered heterocycles.[9]

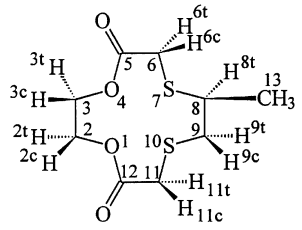

Scheme 1

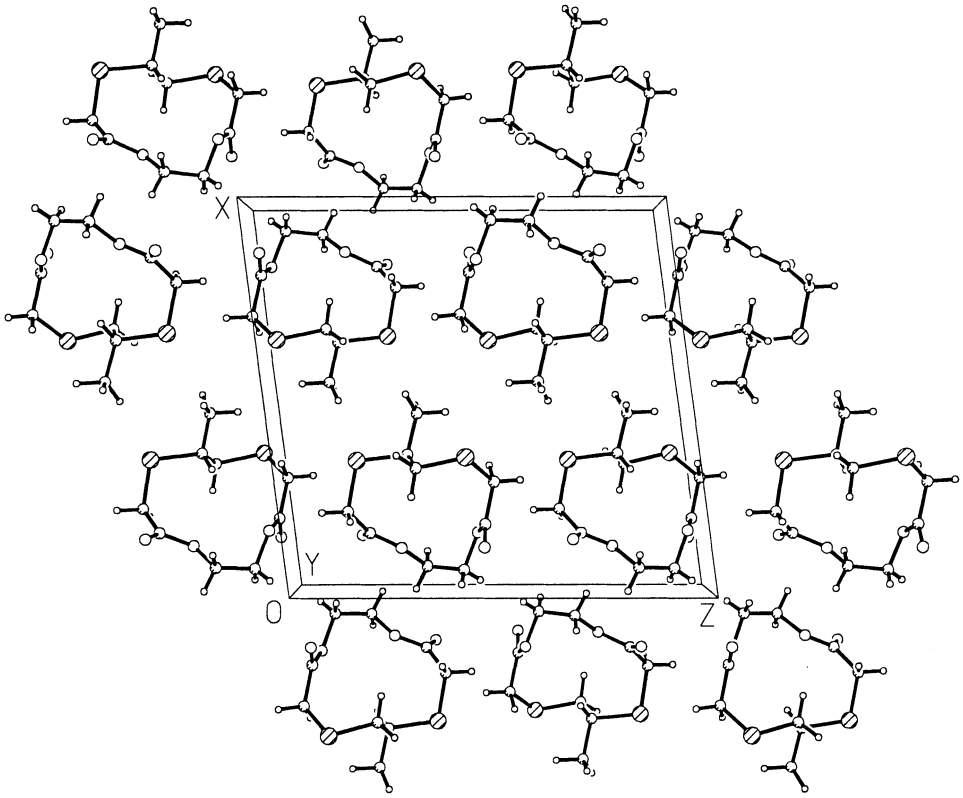

Figure 3. General view of molecular layer of **1** along the *y*-axis

The S—C—C—S torsion angle is the main structural characteristic of the macrocycle **1**. According to the MMX data, all conformers of **1** can be subdivided into three large groups, **A, B** and **C**, with different conformations of this fragment (Scheme 2; see also Table 9). Their Boltzmann populations derived from molecular mechanics energies are 55, 36 and 9% respectively.[5b–d] Each group of conformers can be roughly considered as a single conformational unit ('macroconformer'), because its members possess family similar structures which differ mainly in the terminal torsion angles of the ester moieties (cf. Fig. 4, Table 6). The internal CC(O)— OC bond of the ester fragments appeared to be fixed in the *anti* conformation. In all of the calculated structures the O— C— C— O fragment was strictly *gauche*. Hence both O— C— C— O and ester fragments rigidify the structure of the macrocycle, thus facilitating the conformational study.

This *three-conformers model* was the first step in our approach to the quantitative consideration of the complicated conformational equilibrium for **1** on the basis of the linear system of equations of type (1).[5b–d] The necessary $^{3}J_{HH}$ values H(8*t*)–H(9*c*) and H(8*t*)–H(9*t*) for the **A, B** and **C** macroconformers (J_A, J_B and J_C) were estimated by averaging in the Boltzmann proportions of individual parameters for the calculated conformers within each group.

Useful information can be obtained from the vicinal ^{13}C–^{1}H spin–spin coupling constants.[10,11] We performed a partial analysis of proton-coupled ^{13}C NMR spectrum for solution of **1** in C_6D_6, which provided us with experimental values of vicinal couplings of the methyl carbon atom $^{3}J_{C(13)H(9c)}$ and $^{3}J_{C(13)H(9t)}$ (Table 7 and Table 8). These parameters were also calculated for all 28 individual conformers using the Karplus equation[11], and then we estimated C–H coupling for the **A, B** and **C** macroconformers by averaging with the Boltzmann weight factor within each group. Hence we obtained four vicinal couplings to test the three-conformer equilibrium model for macrocycle **1**. This gave us the

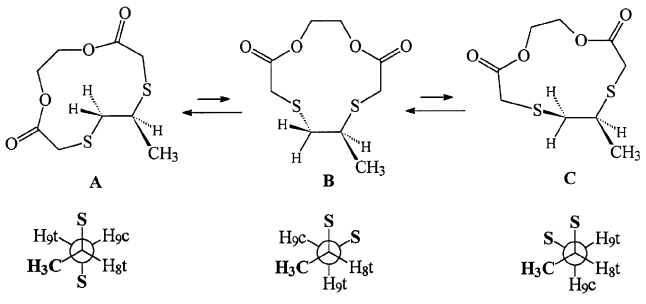

Scheme 2

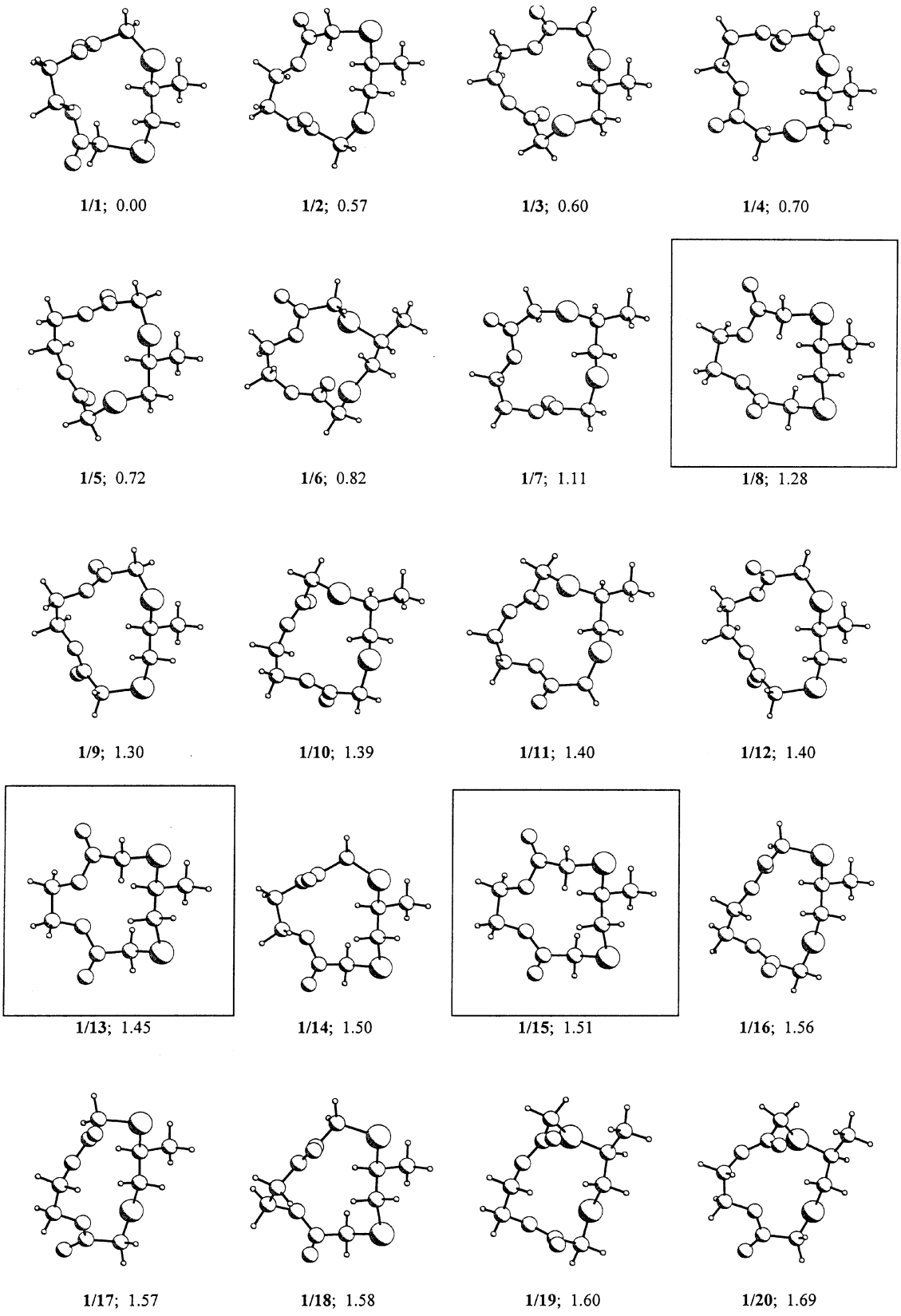

Figure 4. The calculated conformations of (*S*)-**1** and their steric energies (in kcal mol^{-1})

Table 6. Endocyclic torsion angles (°) and steric energy (kcal mol^{-1}) for conformers of (*S*)-***1*** (molecular mechanics[7])

Conformer	*E*	O(1)C(2)	C(2)C(3)	C(3)O(4)	O(4)C(5)	C(5)C(6)	C(6)S(7)	S(7)C(8)	C(8)C(9)	C(9)S(10)	S(10)C(11)	C(11)C(12)	C(12)O(1)	SCCMe
X-ray:		**121.9**	**−61.6**	**164.1**	**−174.5**	**99.1**	**−64.6**	**−61.7**	**−171.8**	**−57.7**	**−57.7**	**129.1**	**−171.8**	**−52.1**
1/1	0.00	−175.2	−59.0	94.4	−172.8	63.2	61.1	−145.0	168.0	−67.2	−52.5	105.1	−177.8	−72.0
1/2	0.57	93.8	−59.3	−175.9	−178.0	106.2	−50.1	−67.7	166.9	−146.7	62.5	62.1	−172.0	−73.8
1/3	0.60	−111.8	63.2	−173.2	179.0	−77.3	96.0	−156.9	65.8	92.1	−73.8	−75.0	175.5	−174.3
1/4	0.70	−175.0	−53.7	104.0	−174.5	78.9	59.4	−167.4	61.8	72.0	−133.2	82.6	−174.6	−177.4
1/5	0.72	−149.2	59.2	73.9	−179.3	53.6	51.7	−166.2	61.0	92.8	−61.4	−64.6	178.1	−178.1
1/6	0.82	102.3	−54.1	−175.5	−175.9	87.9	−131.0	65.7	62.3	−172.5	66.3	75.4	−172.2	−173.1
1/7	1.11	−103.1	54.2	175.1	175.6	−86.1	131.7	−70.9	−57.7	171.3	−66.1	−74.8	172.2	64.9
1/8	1.29	105.1	−57.5	173.2	−179.4	100.0	−66.7	−69.4	−174.0	−56.3	−52.1	143.0	−172.2	−55.9
1/9	1.30	−169.8	58.3	72.6	−177.1	39.5	55.5	−156.6	171.5	−97.0	80.5	−98.6	−178.2	−69.0
1/10	1.39	−73.6	−59.2	149.4	−179.1	65.2	60.7	−94.3	−56.8	168.1	−57.7	−49.2	177.6	65.4
1/11	1.40	174.7	−62.1	111.9	−177.2	76.7	71.2	−93.8	−61.0	160.3	−98.2	73.8	−177.3	61.6
1/12	1.40	−160.8	62.7	−154.8	174.0	−88.0	82.8	−154.1	172.7	−93.4	88.8	−102.7	−177.4	−67.8
1/13	1.45	151.7	−56.1	158.7	−176.5	103.2	−63.7	−59.8	−165.8	−58.5	−64.0	106.4	−176.5	−47.4
1/14	1.50	180.0	−47.3	−76.5	177.8	−113.0	73.6	−125.9	−174.2	−62.7	−56.2	108.4	−174.2	−59.5
1/15	1.51	126.7	−57.2	169.2	−178.8	99.0	−65.2	−64.4	−168.2	−59.2	−57.4	125.9	−174.1	−50.3
1/16	1.56	72.6	57.5	−170.6	−179.0	−98.2	84.8	−96.4	169.2	−160.4	58.4	36.6	−176.2	−72.1
1/17	1.57	−154.7	61.8	−159.3	−179.6	−106.1	94.7	−86.3	169.5	−164.0	83.3	−88.3	173.2	−71.9
1/18	1.58	79.7	50.5	−168.9	177.4	−104.3	70.8	−102.4	−169.7	−63.9	−60.1	124.1	−173.6	−52.0
1/19	1.60	72.3	57.6	−154.3	−179.7	−60.2	−61.5	87.1	63.1	−171.8	58.8	49.8	−177.0	−170.0
1/20	1.69	−175.2	60.9	−113.0	178.8	−75.7	−70.1	85.7	67.4	−164.3	99.4	−73.1	176.4	−166.0
1/21	1.90	−68.9	−51.5	159.4	−173.1	52.3	44.6	−172.4	59.2	86.6	−73.8	−56.9	−173.5	−179.8
1/22	1.90	177.3	−48.0	−74.3	178.1	−90.9	82.8	−166.2	66.5	79.1	−121.7	87.8	−174.1	−173.6
1/23	1.95	−78.7	−60.6	157.7	−171.3	43.8	46.9	−162.0	165.0	−102.8	75.7	−98.6	−170.2	−74.6
1/24	1.96	−164.6	50.0	80.0	−172.4	125.0	−58.3	−71.7	−171.4	−92.6	68.3	−111.2	176.8	−53.4
1/25	1.97	155.0	−64.4	146.1	−177.9	118.1	−90.9	54.7	167.5	−170.0	−59.0	90.9	−176.6	−68.8
1/26	2.04	157.4	−60.7	−79.0	−170.4	−97.8	77.6	−102.2	163.7	−165.8	50.9	39.5	−169.8	−77.2
1/27	2.20	79.7	52.5	−167.9	174.5	−84.3	89.9	−160.8	70.3	83.6	−115.6	98.5	−176.4	−170.4
1/28	2.28	76.5	50.3	−175.7	175.7	−92.9	117.4	−77.1	−61.3	174.2	−89.2	87.5	−173.8	61.5

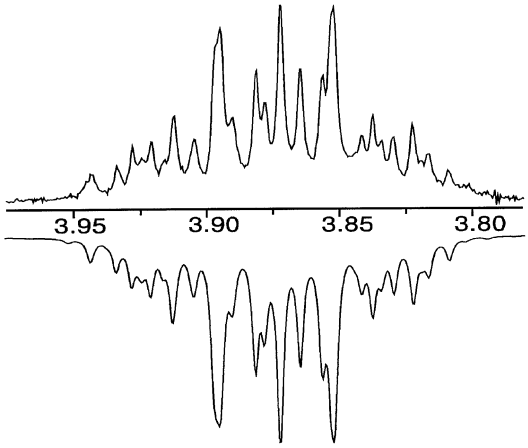

Figure 5. Part of the ^{1}H NMR spectrum of the OCH_2CH_2O moiety (400 MHz, in C_6D_6)

slightly statistically overestimated system of the type (1) of five linear equations with three unknowns.

The weighted least-squares solution of this system has shown that the contribution of macroconformer **C** is statistically insignificant. Weight factors were set equal to 1.0 for spin couplings and 20.0 for the mole fraction equation to take into account the 'rigidity' of the latter. Numerically, the solution with two significant regressors can be presented as follows:

$$J^{\text{exp.}} = 0.78\ (0.02)\ J^{\text{A}} + 0.26\ (0.02)\ J^{\text{B}} \qquad (2)$$

where $J \in \{{}^3J_{\text{H(8t)H(9t)}}, {}^3J_{\text{H(8t)H(9c)}}, {}^3J_{\text{C(13)H(9c)}}, {}^3J_{\text{C(13)H(9t)}}, 1.0\}$, $n^{\text{A}} = 0.78$ and $n^{\text{B}} = 0.26$. The values in parentheses denote standard deviations of estimated mole fractions n^{A} and n^{B}. Within the experimental error limits the total mole fraction is equal to 1. It is worth noting the excellent coincidence of the experimental and calculated couplings, which is probably limited only by the accuracy of molecular modelling and the current approximation of the Karplus equations[11,12] (multiple $R = 0.999$, RMS = 0.25, see Table 8).

The predominance of an *S,S*-transoidal arrangement for the $SCHMeCH_2S$ moiety is not surprising and has literature analogies with some crown thioethers.[1–5] The presence of a methyl group in **1** does not change this regularity.

In the next step of the approach we considered the more detailed *six-conformer model*, taking into account two possible *gauche* rotamers of the C(2)—C(3) bond (Scheme 3).

We studied the four-spin system of the OCH_2CH_2O moiety. The experimental ^{1}H NMR spectrum of this group of protons (400 MHz, see Fig. 5) was fairly well resolved, but extremely tightly coupled, because non-equivalence of these protons was caused only by the very distant methyl group. To analyse the multiplet structure we applied a technique of total lineshape fitting[13,14] within the ABCD spin system.

Particular care ought to be paid to the assignment of those protons, which could not be done on the basis of long-range interproton coupling. We could not recognize the line splittings corresponding to any four- or five-bond interproton coupling constants via the heterocyclic paths. The second-order character of the multiplet also prevents the use of NOE factors for solving the problem. Our assignment was based on the assignment of the carbon framework of the molecule, which was performed using a variety of long-range ^{13}C–^1H coupling constants (see below and Experimental section for numerical values).

The crucial point for the assignment of carbon atoms C(2) and C(3) was the observation of long-range couplings $^4J_{\text{C(2)H(11c)}} = 0.37$ Hz and $^4J_{\text{C(3)H(6c)}} = 0.47$ Hz, which was done with help of *J*-resolved 2D spectra with selective excitation[15] of protons H(11c) and H(6c). These

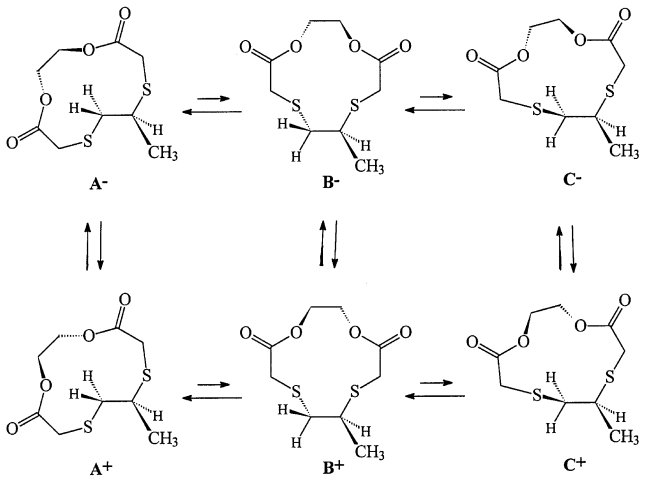

Scheme 3

Table 7. Spin–spin coupling in NMR spectra (Hz)

	$^3J_{HH}$[a]						$^3J_{CH}$[b]								
Conformer	**8t–9c**	**8t–9t**	**2c–3c**	**2t–3c**	**2c–3t**	**2t–3t**	**C(8)H(6c)**	**C(8)H(6t)**	**C(6)H(8t)**	**C(13)H(9c)**	**C(13)H(9t)**	**C(11)H(9c)**	**C(11)H(9t)**	**C(9)H(11c)**	**C(9)H(11t)**
1/1	1.66	12.00	2.83	0.37	10.60	3.09	7.98	2.32	6.09	7.55	3.51	2.71	7.82	7.80	1.23
1/2	1.61	11.91	3.05	0.38	10.58	2.79	1.08	7.70	2.98	7.57	3.56	6.07	0.67	2.47	7.97
1/3	12.32	2.29	2.41	10.34	0.62	2.60	5.80	6.00	5.07	1.87	3.27	5.81	5.62	7.59	3.63
1/4	12.36	2.82	3.48	0.13	10.82	3.76	7.98	2.95	3.71	2.17	2.83	7.58	3.32	1.48	7.15
1/5	12.36	2.75	2.64	10.45	0.61	2.57	7.85	1.36	3.86	2.17	2.87	5.79	5.65	7.97	2.28
1/6	12.36	2.67	3.69	0.14	10.80	3.42	7.24	1.68	7.94	2.00	3.05	3.45	1.61	2.92	7.89
1/7	2.90	3.76	3.43	10.80	0.14	3.68	1.62	7.23	3.57	2.61	7.85	1.64	3.49	7.89	2.90
1/8	3.58	12.28	3.27	0.26	10.66	3.05	2.43	7.95	3.18	7.98	1.87	1.60	7.97	7.82	1.27
1/9	1.94	12.15	2.68	10.45	0.57	2.58	7.95	1.66	4.81	7.69	3.27	6.08	5.34	4.02	7.32
1/10	2.91	3.72	2.62	0.61	10.45	2.57	7.98	2.20	6.16	2.64	7.84	1.40	3.83	7.97	1.92
1/11	3.38	3.27	2.50	0.56	10.42	2.72	7.71	3.34	6.16	2.31	7.93	0.91	4.85	5.54	6.21
1/12	1.98	12.17	2.30	10.15	0.66	2.37	7.15	4.48	5.08	7.74	3.15	5.70	5.78	4.93	6.66
1/13	4.85	11.84	3.12	0.21	10.56	3.08	2.12	7.98	2.16	7.80	1.25	1.74	7.98	7.97	2.19
1/14	3.49	12.29	3.75	0.05	10.85	3.99	7.73	3.28	7.35	7.98	1.93	2.16	7.95	7.91	1.53
1/15	4.42	12.03	3.18	0.25	10.60	3.00	2.28	7.97	2.64	7.89	1.45	1.83	7.98	7.94	1.61
1/16	1.81	12.04	2.66	10.50	0.52	2.76	7.01	4.50	6.25	7.66	3.39	4.55	0.95	1.95	7.98
1/17	1.84	12.09	2.47	10.22	0.59	2.41	6.06	5.58	5.18	7.68	3.30	4.07	1.18	4.56	7.09
1/18	3.98	12.17	3.37	10.74	0.14	3.54	7.83	2.96	6.76	7.95	1.65	2.23	7.94	7.97	1.86
1/19	12.32	2.40	2.75	10.54	0.50	2.78	2.03	7.98	6.76	1.70	3.38	3.50	1.55	2.02	7.98
1/20	12.22	2.00	2.87	10.50	0.48	2.63	2.93	7.79	6.85	1.43	3.80	4.48	1.03	6.33	5.40
1/21	12.35	2.96	3.61	0.18	10.82	3.47	7.53	0.96	3.06	2.33	2.71	6.48	4.93	7.61	3.43
1/22	12.32	2.28	3.69	0.07	10.84	3.91	7.16	4.36	3.95	1.83	3.28	7.08	4.14	2.63	7.44
1/23	1.45	11.75	2.47	0.78	10.30	2.25	7.66	1.09	4.07	7.41	3.86	6.63	4.58	3.41	7.59
1/24	3.68	12.27	3.61	10.77	0.12	3.45	1.70	7.95	3.46	7.97	1.80	5.48	5.96	2.67	7.90
1/25	1.98	12.04	2.19	0.77	10.08	2.25	5.08	6.52	7.85	7.77	3.34	3.57	1.37	7.97	1.90
1/26	1.41	11.71	2.22	0.79	10.28	2.46	7.49	3.63	6.74	7.37	3.92	3.80	1.31	1.40	7.84
1/27	12.20	1.91	3.11	10.67	0.23	3.31	6.51	5.31	4.61	1.57	3.67	6.68	4.68	3.42	7.31
1/28	3.32	3.31	3.39	10.76	0.14	3.58	3.19	7.37	4.31	2.34	7.92	1.81	3.22	6.59	5.23
Average[c]	5.84	7.93	2.95	3.90	7.06	3.01	6.07	4.08	5.06	5.20	3.52	4.16	4.96	5.83	4.24
Experimental[d]	4.84	10.17	2.69	6.47	6.86	2.58	4.82	4.11	3.29	6.18	3.49	3.97	5.16	4.60	4.60

[a] Calculated by PCMODEL program.[7]
[b] Calculated using Karplus-type equation.[11]
[c] Averaged in accordance with the Boltzmann populations of conformers.
[d] Measured for C_6D_6 solution.

Table 8. Experimental and calculated vicinal spin–spin coupling constants J_{HH} and J_{CH} in thiacrown **1** (Hz)

Coupling	Experimental	Calculated Eqn (2)	Eqn (3)	Eqn (4)	Eqn (5)	Eqn (6)
$^3J_{H(8)H(9c)}$	4.84	4.88	5.25	4.94	4.21	4.44
$^3J_{H(8)H(9t)}$	10.17	10.04	10.28	9.07	9.77	9.99
$^3J_{H(2c)H(3c)}$	2.69	—	3.03	2.85	2.73	2.81
$^3J_{H(2t)H(3c)}$	6.47	—	5.72	3.30	5.26	4.80
$^3J_{H(2c)H(3t)}$	6.86	—	6.12	7.35	5.39	5.66
$^3J_{H(2t)H(3t)}$	2.58	—	3.09	2.91	2.78	2.79
$^3J_{C(Me)H(9c)}$	6.18	6.48	6.65	5.88	6.30	6.48
$^3J_{C(Me)H(9t)}$	3.49	3.21	3.35	3.02	3.01	2.48
$^3J_{C(8)H(6c)}$	4.82	—	—	5.93	5.88	5.59
$^3J_{C(8)H(6t)}$	4.11	—	—	3.98	4.22	4.37
$^3J_{C(6)H(8)}$	3.29	—	—	4.93	4.93	3.79
$^3J_{C(11)H(9c)}$	3.97	—	—	4.11	4.12	4.57
$^3J_{C(11)H(9t)}$	5.16	—	—	5.10	5.22	5.74
$^3J_{C(9)H(11c)}$	4.60	—	—	5.64	5.85	4.90
$^3J_{C(9)H(11t)}$	4.60	—	—	4.03	4.04	5.00
Σn^i	1.0[a]	1.04	1.08	0.97	0.97	0.96
$(N+1)$[b]	—	5	9	16	16	16
R[c]	—	0.999	0.997	0.979	0.987	0.991
RMS[d]	—	0.25	0.56	1.11	0.88	0.77

[a] Assumed.
[b] Number of equations (sets).
[c] Multiple correlation coefficient.
[d] Root mean square deviation of experimental and calculated values.

Table 9. Consecutive formal classification of conformers into groups (macroconformers)

Three-conformer model	Six-conformer model	Sixteen-conformer model	Calculated conformers
A	$\mathbf{A}^-$	$\mathbf{A1}^-$	**1, 14**
		$\mathbf{A2}^-$	**2**
		$\mathbf{A3}^-$	**8, 13, 15**
		$\mathbf{A4}^-$	**23, 26**
		$\mathbf{A5}^-$	**25**
	$\mathbf{A}^+$	$\mathbf{A1}^+$	**9, 12**
		$\mathbf{A2}^+$	**16, 17**
		$\mathbf{A3}^+$	**18**
		$\mathbf{A4}^+$	**24**
B	$\mathbf{B}^-$	$\mathbf{B1}^-$	**4, 22**
		$\mathbf{B2}^-$	**6**
		$\mathbf{B3}^-$	**21**
	$\mathbf{B}^+$	$\mathbf{B1}^+$	**3, 5**
		$\mathbf{B2}^+$	**19, 20**
C	$\mathbf{C}^-$	$\mathbf{C1}^-$	**10, 11**
	$\mathbf{C}^+$	$\mathbf{C1}^+$	**7, 28**

data are in good agreement with our earlier experiments on cyclohexane.[10] Further, one-bond ^{13}C–^1H connectivities obtained by HETCOR provided an unambiguous assignment of the H(2) and H(3) protons, and also starting values of their chemical shifts. Total lineshape fitting was performed with the NMRCON program.[13] The technique of gradual smoothing of the lineshape (details of the procedure will be published elsewere) resulted in a one-grand cycle-go solution. The calculated spectrum (Fig. 5) is in good coincidence with the experimental one: the *R*-factor of 0.984 allowed the estimation of spin–spin coupling constants at an accuracy level of 0.01 Hz and better. Final values of chemical shifts and coupling constants are presented in the Experimental section, and four vicinal coupling constants, $^3J_{H(2c)H(3c)}$, $^3J_{H(2c)H(3t)}$, $^3J_{H(2t)H(3c)}$ and $^3J_{H(2t)H(3t)}$, are also presented in Table 7 and Table 8. Together with the other four vicinal couplings [see Eqn (2)], we have a system of nine linear equations ($N = 8$), which was used to study the equilibrium in terms of the six-conformers model ($\mathbf{A}^-$, $\mathbf{A}^+$, $\mathbf{B}^-$, $\mathbf{B}^+$, $\mathbf{C}^-$ and $\mathbf{C}^+$; Scheme 3, Table 9). The $-$ and $+$ signs denote the sign of the OCCO torsional angle. The weight factors were set equal to 1.0 for spin couplings and 10.0 for the mole fraction equation. The $^3J_{HH}$ and $^3J_{CH}$ values for the $\mathbf{A}^-$, $\mathbf{A}^+$, $\mathbf{B}^-$, $\mathbf{B}^+$, $\mathbf{C}^-$ and $\mathbf{C}^+$ macroconformers were estimated by averaging in the Boltzmann proportions of parameters for the calculated conformers within each group. The weighted least-squares solution of this system showed that the contribution of macroconformers $\mathbf{B}^-$, $\mathbf{C}^-$ and $\mathbf{C}^+$ is statistically insignificant. Numerically the resulting solution with three significant regressors can be presented as follows:

$$J^{exp} = 0.55\ (0.04)\ J^{A^-} + 0.25\ (0.05)\, J^{A^+} + 0.28(0.04)\ J^{B^+} \quad (3)$$

which shows that the most populated macroconformer is $\mathbf{A}^-$. Note, that the mole fractions obtained from this solution correspond perfectly to the less detailed ones from Eqn (2).

In the final stage of our investigation, we performed a complete study of the proton-coupled ^{13}C NMR spectrum so as to maximize the experimental information via the vicinal spin–spin coupling network around the macrocycle. A variety of ambiguities were cleared up by selective double resonance experiments and two-dimensional *J*-resolved spectra with selective excitation.[15] This allowed us to obtain another set of seven ^{13}C–^{1}H vicinal spin–spin coupling constants: $^{3}J_{C(8)H(6c)}$, $^{3}J_{C(8)H(6t)}$), $^{3}J_{C(6)H(8t)}$, $^{3}J_{C(11)H(9c)}$, $^{3}J_{C(11)H(9t)}$), $^{3}J_{C(9)H(11c)}$ and $^{3}J_{C(9)H(11t)}$ (see Experimental section and Table 7 and Table 8). Hence from this step we have a total of 15 vicinal spin couplings, which is the maximum possible for the spin coupling network of macrocycle **1**.

With these data at hand in principle we could raise the level of the conformational model under consideration up to 16 conformers. To achieve this we continued the subdivision of 28 calculated conformers into smaller groups of geometrically related forms: **A1**^{1}, **A2**$^{-}$, **A3**$^{-}$, **A4**$^{-}$, **A5**$^{-}$, **A1**$^{+}$, **A2**$^{+}$, **A3**$^{+}$, **B1**$^{-}$, **B2**$^{-}$, **B1**$^{+}$, **B2**$^{+}$, **C1**$^{-}$ and **C1**$^{+}$ (Table 9).

The further subdivision was not so evident as in the three and six-conformer models. We used both torsional angles (Table 6) and spin coupling values (Table 7 and Table 8) to group the calculated conformers into less numerous experimentally detectable ones (macroconformers). The resulting distribution is summarized in Table 9. However, the statistical treatment of the resulting set of equations (1) ($N = 15$) did not lead to any self-consistent solution. Obviously this was the result of the accumulation of uncertainties in the course of structural and spectral calculations. Most probably the Karplus equation used[11] did not afford accurate $^{3}J_{CH}$ values for the C–S–C–H fragments. Thus, the additional seven parameters taken into consideration did not permit the evaluation of the population of the theoretically possible number of conformers.

Moreover, the use of this set of experimental data for the three- and six-conformer models (Schemes 2 and 3) gave solutions (4) and (5), respectively, with increased standard deviations of estimated conformer populations:

$$J^{\text{exp.}} = 0.70\ (0.07)\ J^{\text{A}} + 0.28\ (0.08)\ J^{\text{B}} \qquad (4)$$

$$J^{\text{exp.}} = 0.49\ (0.06)\ J^{\text{A}^-} + 0.29\ (0.08)\ J^{\text{A}^+} + 0.20\ (0.06)\ J^{\text{B}^+} \qquad (5)$$

where $J \in \{^{3}J_{(1)}, {}^{3}J_{(2)}, \ldots, {}^{3}J_{(15)}, 1.0\}$

We simplified the 16 conformer model, decreasing step by step the number of conformers: expelling the least stable one and then applying the statistical procedure. The final stable solution with only three statistically significant regressors was as follows:

$$J^{\text{exp.}} = 0.33\ (0.05)\ J^{\text{A3}^-} + 0.46\ (0.05)\ J^{\text{A1}^+} + 0.18\ (0.05)\ J^{\text{B1}^-} \qquad (6)$$

The accuracy of this equation ($R = 0.991$ and RMS = 0.77, see Table 8) is reasonable. It is important that one of the most significant regressors corresponds to the conformer **A3**$^{-}$, which is equivalent to the solid-state x-ray structure of the macrocycle **1**. However, in benzene solution this conformer is not the only one. Moreover, it is not the major one.

It is worth mentioning that the described estimations do not depend critically on the calculated relative stability of possible conformers. The spectral parameters (coupling constants) for each macroconformer are obtained by averaging of spectral parameters for calculated conformers within the group according to their energy, in Boltzmann proportions. Hence the coupling constants for the macroconformer would depend on the relative stability of the conformers, and consequently on parametrization of the force field (or quantum chemistry method) used for calculation. However, this dependence is not substantial, because the macroconformers are formed from calculated conformers possessing as similar geometrical and spectral parameters as possible (Tables 6, 7 and 9). The dependence is then essentially smoothed over by correlation of experimental NMR parameters with statistically weighted NMR parameters of the macroconformers. The more detailed is the classification of conformers into groups, the closer is each macroconformer to any single calculated conformer, and the weaker is the dependence of estimated coupling constants for the macroconformer on the relative energies of its components. Finally, if one had a number of experimentally determined NMR parameters equal to or exceeding the number of calculated conformers under consideration, each macroconformer would consist of only one conformer. Then the experimental estimation of their population should not depend on the calculated relative stability at all. The results of the exploration of the 16-conformer model [Eqn. (6)] seem to support this conclusion.

Thus, in particular cases the combination of x-ray crystal structure analysis, NMR spectroscopy and computational methods allows a fairly complete analysis of the conformational structure and distribution for such difficult objects as macroheterocycles. Further improvement in experimental conformational determinations can be achieved by more detailed consecutive formal classifications of conformer groups along with use of more NMR spectral parameters (NOE factors, etc.), and by advances in methods for the calculation of structural and spectral parameters. *Inter alia*, improvements in calculations can be achieved by consideration of the influence of the solvent on the relative stability and geometry of conformers.

General approach to the estimation of the population of conformers in solution

Generalization of the approach used for conformational

analysis of macrocycle **1** permits the general principles of the estimation of conformer population in solution to be formulated. They are as follows:

1. Generation of all possible conformers and calculation of their structural parameters and energy.
2. Calculation of spectral parameters for these conformers (i.e. J_{HH}, J_{CH}).
3. Consecutive formal classification of these conformers into groups (macroconformers), leading to various conformational models of the system with different numbers of participating macroconformers.
4. Estimation of spectral parameters for these macroconformers by averaging within each group (in Boltzmann proportions) of individual parameters of calculated conformers.
5. Experimental determination of the maximum number of time-averaged spectral parameters (i.e. J_{HH}, J_{CH}).
6. Setting up of a statistically overestimated system of linear equations describing the experimental parameters as a sum of weighted calculated (in step 4) parameters of macroconformers.
7. Statistical solution of this system affording the macroconformer populations for the selected model of equilibrium.

In principle, this protocol can be applied to any multicomponent chemical equilibrium: conformational, isomerizational, tautomeric, etc.

EXPERIMENTAL

Crown thioether **1** was obtained from ethylene glycol bis(mercaptoacetate) and methylacetylene by one-step homolytic cycloaddition of α ,ω-dithiols to alkynes as described earlier.[6]

NMR spectra were recorded on a Varian VXR-400 spectrometer (400 MHz for protons) at 298 K for 0.1–0.2 M solutions in C_6D_{12}, C_6D_6, $CDCl_3$, CD_3OD and CD_3CN. Assignment of signals was based on double-resonance and HETCOR experiments. The final assignment of ^{13}C NMR signals and ^{13}C–H long-range spin–spin couplings was made with the help of the heteronuclear two-dimensional *J*-resolved spectra with selective excitation[15] using the SEL2DJ pulse sequence.[16] The analysis of the H(6), H(8), H(9) and H(11) signals and the analysis of the proton-coupled ^{13}C NMR multiplets were performed with a first-order approach. The protons H(2) and H(3) revealed highly coupled multiplets for all the solvents used. The total lineshape analysis of that part of spectrum (for solution in C_6D_6) was performed using the NMRCON program[13] adopted for an IBM PC. The calculations were performed in terms of the ABCD spin system. Starting parameters for proton chemical shifts were accepted from the high-resolution HETCOR experiment with a digital resolution of 0.5 Hz per point on the proton chemical shift axis. A series of gradually diminishing smoothing of the experimental lineshape was used for a steady convergence of iterative process. An initial Lorentzial broadening factor of 6 Hz allowed the χ^2 surface to be smoothed sufficiently. Then a stepwise series of broadening factors of 4.0, 3.0, 2.0, 1.0, 0.5 and 0.0 Hz was applied within the grand cycle (see also the discussion in Ref. 14).

The parameters of the ^1H NMR spectra for the crown thioether **1** (solution in C_6D_6) were as follows (δ, ppm): H(Me) 1.211 [ddd,3H,$J_{H(Me)H(8)}$ = 6.79 Hz,$J_{H(Me)H(9c)}$ = 0.46 Hz]; H(2) and H(3) 3.80–3.95 (m, 4H), H(2c) 3.921 m, H(2*t* 3.846, H(3*c* 3.903, H(3*t* 3.859 [$J_{H(2c)H(2t)}$= 12.21 Hz,$J_{H(2c)H(3c)}$ = 2.58 Hz,$J_{H(2c)H(3t)}$ = 6.86 Hz,$J_{H(2t)H(3c)}$ = 6.47 Hz and $J_{H(3c)H(3t)}$ = −12.11 Hz); H(6*c*) 2.976 [d,1H,$J_{H(6c)H(6t)}$ = 14.26 Hz]; H(6*t*) 2.795 (d, 1H); H(8) 3.036 [ddq,1H,$J_{H(8)H(9c)}$ = 4.84 Hz,$J_{H(8)H(9t)}$ = 10.17 Hz]; H(9*c*) 2.923 [ddq,1H,$J_{H(9c)H(9t)}$ = −13.58 Hz]; H(9*t*) 2.308 (dd, 1H); H(11*c*) 2.809 [d,1H,$J_{H(11c)H(11t)}$ = 14.06 hz]; H(11t) 2.742 (d, 1H).

The multiplicity of the proton-coupled ^{13}C NMR spectrum was complex for all the signals of crown thioether **1**. Numerical estimates of ^{13}C–H spin–spin couplings were obtained by the first-order analysis of a proton-coupled ^{13}C NMR spectrum and of a series of spectra with selective decoupling of the following signals: methyl group, H(8), H(9*c*), and H(9*t*). Direct estimates of a series of ^{13}C–H long-range spin–spin coupling constants were found using *J*-resolved two-dimensional ^{13}C NMR spectra with selective excitation of H(6*c*), H(8), H(9*c*), H(9*t*) and H(11*c*) protons. No special experiments were performed to assign the tertiary carbons and the ^{13}C–H one-bond coupling constants. The parameters of ^{13}C NMR spectra for the crown thioether **1** (solution in C_6D_6) were as follows (δ, ppm): C(2) 61.70 [$^1J_{C(2)H(2)}$ = 148.88 Hz,$^4J_{C(2)H(11c)}$ = 0.37 Hz], C(3) 61.81 [$^1J_{C(3)H(3)}$ = 148.31 Hz,$^4J_{C(3)H(6c)}$ = 0.47 Hz], C(5) and C(12) are 169.59 and 169.72, C(6) 32.50 [$^1J_{C(6)H(6c)}$ and $^1J_{C(6)H(6t)}$ = 136.02 and 138.92 Hz,$^3J_{C(6)H(8)}$ = 3.29 Hz], C(8) 39.47 [$^1J_{C(8)H(8)}$ = 141.34 Hz,$^2J_{C(8)H(9c)}$ = 4.11 Hz,$^2J_{C(8)H(9t)}$ = 4.03 Hz,$^3J_{C(8)H(6c)}$ = 4.82 Hz,$^3J_{C(8)H(Me)}$ = 5.68 Hz], C(9) 39.09 [$^1J_{C(9)H(9c)}$ and $^1J_{C(9)H(9t)}$ = 138.94 and 142.24 Hz,$^2J_{C(9)H(8)}$ = 4.60 Hz,$^2J_{C(9)H(Me)}$ = 5.68 Hz,$^3J_{C(9)H(11c)}$ = 4.60 Hz,$^3J_{C(9)H(11t)}$ = $^3J_{C(9)H(11c)}$ = 4.60 Hz], C(11) 33.18 [$^1J_{C(11)H(11c)}$ and $^1J_{C(11)H(11t)}$ = 138.98 and 136.97 Hz,$^3J_{C(11)H(9c)}$ = 3.97 Hz,$^3J_{C(9)H(9t)}$ = 5.16 Hz].

X-ray study of ***1****.* The structure was solved by the direct method and refined by the full-matrix least-squares technique in anisotropic approximation for non-hydrogen atoms. Hydrogen atoms, located objectively in the difference Fourier map, were refined in isotropic approximation. The final discrepancy factors were $R = 0.075$ and $R_w = 0.102$ for 1315 unique reflections with $I \geq 2.5\sigma$ (I).

Acknowledgements

The authors acknowledge the support of this study by INTAS (Grant 94-1914) and the Russian Foundation for Basic Research (Grant 94-03-09296).

REFERENCES

1. (a) R. M. Izatt, J. S. Bradshaw, S. A. Nielsen, J. D. Lamb, J. J. Christensen and D. Sen. *Chem. Rev.* **85,** 271 (1985); (b) S. R. Cooper. *Acc. Chem. Res.* **21,** 141 (1988); (c) W. N. Setzer and R. S. Glass. *Conformational Analysis of Medium-Sized Ring Heterocycles*, Chapt. 4. VCH Deerfield Beach, FL (1988); (d) W. N. Setzer, E. L. Cacioppo, G. J. Grant and R. S. Glass. *Phosphorus Sulfur Silicon* **45,** 223 (1989); (e) S. R. Cooper and S. C. Rawle. *Struct. Bonding (Berlin)* **72,** 1 (1990); (f) A. J. Blake and M. Schröder. *Adv. Inorg. Chem.*, **35,** 1 (1990); (g) J. M. Desper, D. R. Powell and S. H. Gellman. *J. Am. Chem. Soc.* **112,** 4321 (1990); (h) A. J. Blake, A. J. Holder, G. Reid and M. Schröder. *J. Chem. Soc., Dalton Trans.* 627 (1994); (i) N. R. Champness, S. R. Jacob, G. Reid and C. S. Frampton. *Inorg. Chem.* **34,** 396 (1995).
2. J. C. Lockhart and N. P. Tomkinson. *J. Chem. Soc., Perkin Trans. 2* 533 (1992); J. C. Lockhart, D. P. Mousley, M. N. Stuart Hill, N. P. Tomkinson, F. Teixidor, M. P. Almajano, L. Escriche, J. F. Casabo, R. Sillanpää and R. Kivekäs. *J. Chem. Soc. Dalton Trans.* 2889 (1992); J. D. Holbrey, P. B. Iveson, J. C. Lockhart, N. P. Tomkinson, F. Teixidor, A. Romerosa, C. Viñas and J. Rius. *J. Chem. Soc., Dalton Trans.* 1451 (1993); G. A. Forsyth and J. C. Lockhart. *J. Chem. Soc., Dalton Trans.* 2243 (1994).
3. J. Beech, P. J. Cragg and M. G. B. Drew. *J. Chem. Soc., Dalton Trans.* 719 (1994).
4. W. N. Setzer, E. L. Cacioppo, Qin Guo, G. J. Grant, D. D. Kim, J. L. Hubbard and D. G. VanDerveer. *Inorg. Chem.* **29,** 2672 (1990); W. N. Setzer, Q. Guo, E. J. Meehan and G. J. Grant. *Heteroatom Chem.* **1,** 425 (1990);
5. (a) E. I. Troyansky, R. F. Ismagilov, V. V. Samoshin, Yu. A. Strelenko, D. V. Demchuk, G. I. Nikishin, S. V. Lindeman, V. N. Khrustalyov and Yu. T. Struchkov. *Tetrahedron* **51,** 11431 (1995); (b) V. V. Samoshin. *Abstracts of 17th International Symposium on the Organic Chemistry of Sulfur,* Tsukuba, Japan, 14 (1996); (c) V. V. Samoshin and E. I. Troyansky. *Books of Abstracts, 213th American Chemical Society National Meeting, San Francisco*, Part 2, ORGN 354 (1997); (d) V. V. Samoshin and E. I. Troyansky. *Phosphorus Sulfur Silicon* **120/121,** 181 (1997).
6. D. V. Demchuk, M. I. Lazareva, S. V. Lindeman, V. N. Khrustalyov, Yu. T. Struchkov, R. F. Ismagilov, E. I. Troyansky and G. I. Nikishin. *Synthesis* 307 (1995).
7. *PCMODEL 3.2.* Serena Software, Bloomington, IN, USA.
8. H. Goto. *Tetrahedron* **48,** 7131 (1992).
9. P. S. Son, T.-Y. Lin, T. Grzhybovski, N. H. Cromwell and C. A. Kingsbury. *J. Chem. Soc., Perkin Trans. 2* 313 (1991).
10. V. A. Chertkov and N. M. Sergeev. *J. Am. Chem. Soc.* **99,** 6750 (1977).
11. R. Aydin and H. Günther. *Magn. Reson. Chem.* **28,** 448 (1990).
12. C. A. G. Haasnoot, F. A. A. M. De Leeuw and C. Altona. *Tetrahedron* **36,** 2783 (1980); C. A. G. Haasnoot. *J. Am. Chem. Soc.* **115,** 1460 (1993).
13. J. Heinzer. *J. Magn. Reson.* **26,** 301 (1977).
14. D. S. Stephenson and G. Binsch. *J. Magn. Reson.* **37,** 395, 409 (1980).
15. A. Bax and R. Freeman. *J. Am. Chem. Soc.* **104,** 1099 (1982).
16. V. A. Chertkov. *Abstracts of IX Ampère Summer School*, Novosibirsk, 133 (1987).
17. W. Robinson and G. M. Sheldrick. *Crystallographic Computing Techniques and New Technologies*, p. 366. Oxford University Press, Oxford (1988).

